



PAPER

A method for measuring porosity in the bones using electrical impedance tomography

RECEIVED
14 August 2025REVISED
26 November 2025ACCEPTED FOR PUBLICATION
27 January 2026PUBLISHED
5 February 2026Miguel-Ángel San-Pablo-Juárez^{1,2,3,*} , Maria-Montserrat Oropeza-Saucedo^{1,2} 
and Eduardo Morales-Sánchez³ ¹ Engineering Department, Universidad Interamericana, Puebla, Mexico² School of Engineering, Universidad De Las Américas Puebla, Puebla, Mexico³ CICATA Unidad Querétaro, Instituto Politécnico Nacional, Querétaro, Mexico

* Author to whom any correspondence should be addressed.

E-mail: miguelangel.sanpablo@gmail.com**Keywords:** electrical conductivity, bone density, bone electrical density, osteoporosis

Abstract

Objective. This paper describes a new method for measuring human bone density based on the measurement of bone electrical conductivity (BEC) using the well-known technique: electrical impedance tomography (EIT). **Approach.** The hypothesis is that BEC is directly related to bone mineral density. The proposed method consists of measuring the EIT, and then obtaining the conductivity values of the bones, and take this value to associate this one to a level of porosity. A model of skin, muscle, and bone was developed using computer simulation to vary the porosity in bones and obtain an inverse model in the form of an equation to measure three levels of porosity. **Main results.** The behavior of different porosity levels was simulated, and impedance tomography was applied; it is shown that electrical conductivity varies according to bone porosity. A relationship was subsequently obtained between the measurement of conductivity and bone density, creating a new non-invasive method for possible application to early detection of osteoporosis. **Significance.** This is a novel, non-invasive method for possible application on the early detection of osteoporosis at three different levels of bone porosity.

1. Introduction

Osteoporosis is a bone disease characterized by low bone mass and tissue deterioration, with increased bone fragility and a higher risk of fractures (Muñoz *et al* 2010). It is a preventable process and treatments exist, but it is a silent disease, as the first symptom is often a fracture.

In the world, this disease affects both men and women. This means that one in five women and one in 11 men will suffer from it in their lifetime (Reza 2016).

The study to determine the porosity in the bones is a measurement of bone mass density and currently this type of measurements are performed with a technique called bone densitometry, a method that is also known as dual energy x-ray absorptiometry, the technique is used to measure bone mineral density (BMD) and is considered the standard in the diagnosis of osteoporosis (Mishra *et al* 2011, Vijay *et al* 2011). This technique uses radiation to obtain an x-ray image and then, using software, a measure of BMD is determined based on the approximation of bone mass and area.

Other techniques have been used to measure bone density, such as ultrasound (Turner *et al* 1995, Mautalen *et al* 1995, Baroncelli 2008), which applies acoustic waves at a specific frequency and scans the density based on the images reconstructed on a screen. This technique is rarely used today due to the low resolution of the image and the fact that the diagnosis depends on the radiologist's experience in image analysis.

Another technique for determining bone porosity is impedance spectroscopy, which takes a bone sample and determines the density by comparing the density using x-ray diffraction with the measurement of electrical impedance at different frequencies, and then using equivalent circuits to

obtain a characteristic impedance. There are reports in the literature on this technique where measurements are made on a physical sample of bone, resulting in an invasive technique (Ireta 2012). Some recent research uses electrical impedance spectroscopy to find porosity in bovine bone (Ain *et al* 2024).

Electrical impedance tomography (EIT) has been used to reconstruct images of internal parts of the human body, such as the lungs, chest, heart, brain, and other parts (Holder 2005). This technique makes it suitable for *in vivo* measurements, having the advantage that it does not use ionizing radiation. The EIT technique is based on the fact that when an electric current is applied to two electrodes on the skin, the electric current is distributed internally through skin, muscle, and bone, inducing electrical potentials around the skin with a pattern characteristic of the internal materials (muscle and bone). The induced potentials are directly related to the conductivity of the muscle and the conductivity of the bone.

Osteoporosis is a bone disorder that makes bones fragile and predisposes a person to an increased risk of fracture. It is the most common bone disorder affecting humans (North American Menopause Society 2010). Bone porosity is a loss of bone mass in regions within the spongy bone. These are not hollows or pores of a certain shape, but rather spaces where solid bones are no longer regenerated. The spaces that represent a pore or hole when bone mass is lost are filled with organic fluids with a higher conductivity than bone tissue (Geddes and Baker 1967). We propose that when a bone presents osteoporosis, its electrical conductivity increases because the bone has large pores filled with high-conductivity red bone marrow instead of low-conductivity bone tissue, obtaining a new method to measure osteoporosis by measuring electrical conductivity.

Therefore, in this work, a new noninvasive method for measuring bone density is proposed based on the measurement of electrical conductivity using EIT.

The immediate application of this new noninvasive method for measuring bone electrical conductivity (BEC) is to provide a method for early pre-diagnosis of osteoporosis, at three possible levels: healthy, osteopenia, or osteoporosis. The term ‘early pre-diagnosis’ refers to the fact that this method does not replace the standard method; rather, because it is rapid, noninvasive, simple, and radiation-free, it can be used as a preventive measure.

2. Methods

To develop and test the feasibility of the proposed new method, the following methodology was used:

First, a mathematical solution was found to the problem of reconstructing an electrical conductivity distribution using EIT. This requires solving the governing equation, which is a second-order nonlinear differential elliptic equation. Given the measurement of potential differences across external electrodes connected to the skin surface, the conductivity distribution in human bone must be calculated. The solution was implemented computer-aided, generating a computer model of skin, muscle, and bone. Using this model, simulations were then performed to determine the induced voltages when the bone porosity value varies. A graphical method was developed that displays conductivity as a function of bone porosity. Based on the developed model and the simulations of porous bone, the direct relationship between the measured conductivity and bone porosity was determined. The results were verified using test cells, experimentally applying EIT. Finally, an expression was developed that correlates bone porosity with bone’s electrical conductivity. This expression allows us to conclude that a new method for measuring osteoporosis has been developed.

2.1. EIT

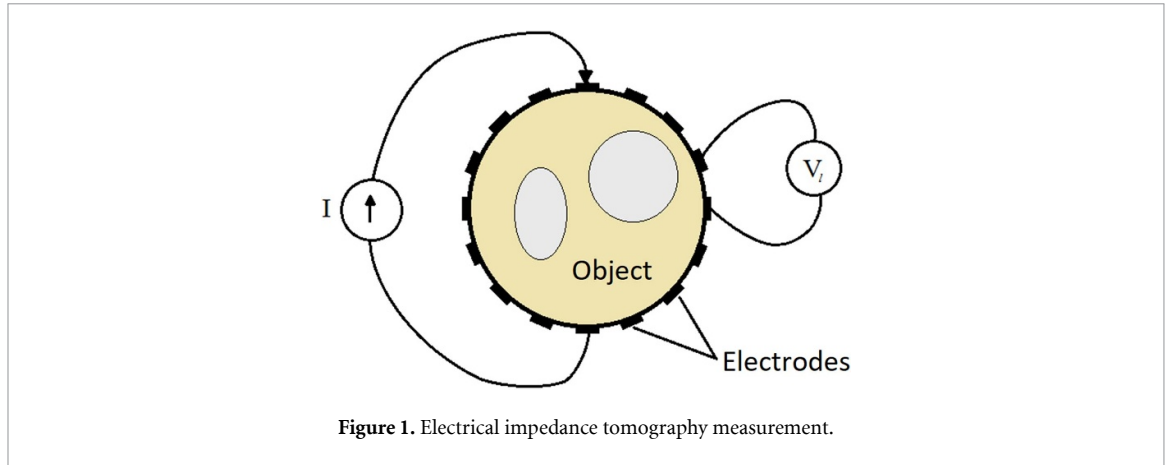
EIT is a method for reconstructing images of the electrical conductivity distribution within an electrically conductive object by injecting a current and measuring the resulting electrical potential at the object’s surface (Molinari 2003). Figure 1 illustrates the application of EIT to a region.

The governing equation in EIT is:

$$\nabla \cdot \sigma \varphi(x, y) = 0. \quad (1)$$

For an electrical conductivity σ , and the resulting potential measured at the object surface φ . It is a second-order nonlinear differential equation equivalent to the generalized Laplace equation (Mueller and Siltanen 2012).

The EIT method consists of applying low-frequency electric current I to a pair of electrodes and measuring the potential difference across each remaining pair of electrodes, then injecting the electric current into the next pair of electrodes and measuring the potential again across the other pairs of electrodes, until all the existing pairs of electrodes have been injected with electric current (Vauhkohonen 2004). Current injection can typically be done between opposite electrodes or between neighboring



electrodes. Once all current injections have been made, the read potentials V_i are stored in a data matrix for processing and reconstruction into an electrical conductivity distribution. This reconstruction is performed by solving the governing equation (1) using a forward and inverse solution reconstruction method. The forward and inverse solutions are well-known techniques in the EIT field, and there are different solution methods for each problem (Holder 2005).

2.2. Backprojection solution

The equipotential back-projection method (also called the Sheffield back-projection method) is a conductivity reconstruction method in EIT that uses the linearization of equation (1) (Barber and Brown 1984). The most widely used algorithm for performing the back-projection is the one described in (Santosa and Vogelius 1990). Equation (1) is linearized as follows:

$$\nabla^2 \phi_p = \nabla \ln(\sigma) \cdot \nabla \phi_u \quad (2)$$

where ϕ_p is a known potential for an initial reference conductivity, ϕ_u is a perturbation of that potential, and σ is the electrical conductivity (Rosell 1989).

Electrical conductivity using the equipotential backprojection method is calculated as

$$\sigma_e = B_M \cdot V_e. \quad (3)$$

With σ_e the conductivity in a division element of the region to be measured, B_M a back projection matrix and V_e the potential at the electrode.

2.3. Data processing for obtaining conductivity

Data processing is carried out in a program compiled in Visual C++, where the solution is programmed using back projection. In this case, the electrical potential is acquired as follows:

$$V_e = \left\{ (v_1^1 v_2^1 \dots v_{13}^1)^T, (v_1^2 v_2^2 \dots v_{13}^2)^T, \dots, (v_1^{16} v_2^{16} \dots v_{13}^{16})^T \right\}. \quad (4)$$

Where V_e are the potential measurements made with an EIT scanner in packets of 13 measurements per current injection. Since in this case the scanner would have 16 electrodes, the current injection is performed 16 times with a total of 208 measurements. Thus, equation (3) becomes

$$[\sigma_e]_{(912 \times 1)} = [B_M]_{(912 \times 208)} \cdot [V_e]_{(208 \times 1)}. \quad (5)$$

With B_M , the back-projection matrix of (Barber and Brown 1984), V_e represents the potential in equation (4), measured with an EIT tomograph, and σ represents the conductivities to be calculated.

Once programmed, a total of 912 conductivity values will be obtained, representing a map of conductivity values. These are arranged in a circular area representing the measured section. Each conductivity is saved in a record for later use. Since back-projection is based on calculations relative to a measurement reference, the calculated values are normalized to a known homogeneous conductivity reference; in this case, this value is 1 S m^{-1} . With normalized values, there are positive and negative conductivity values; therefore, the calculated values are processed to calibrate the measurement and subtract the reference values, thus obtaining only positive values in units of Siemens per meter (S m^{-1}).

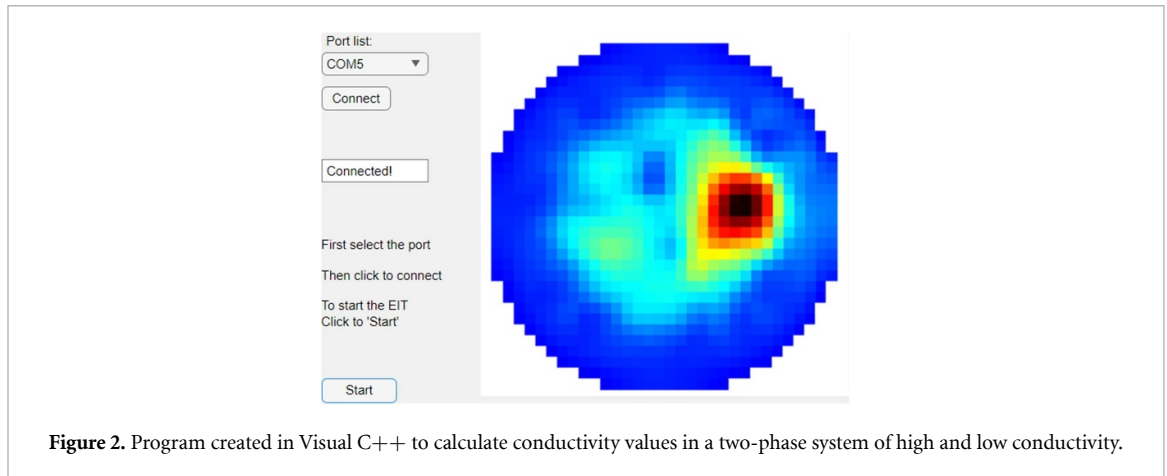


Figure 2. Program created in Visual C++ to calculate conductivity values in a two-phase system of high and low conductivity.

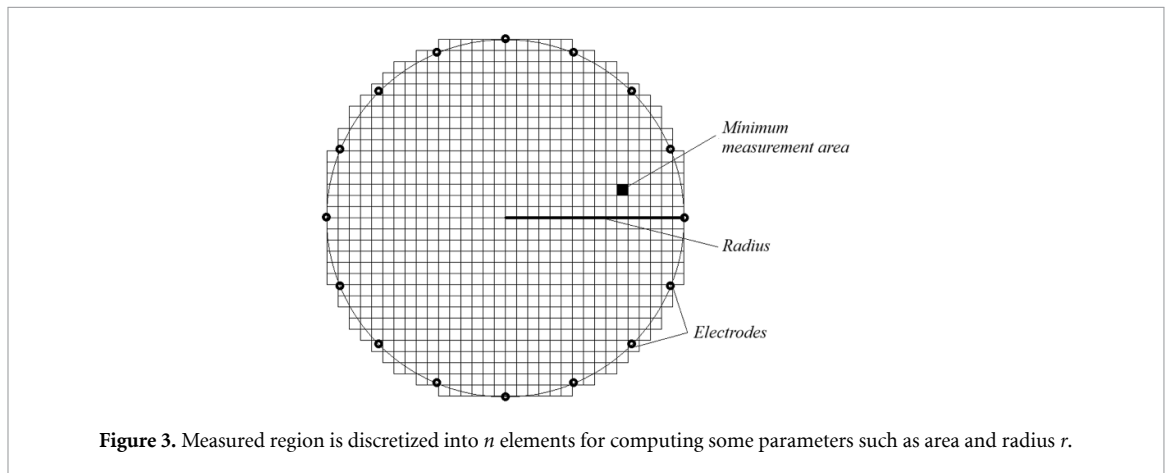


Figure 3. Measured region is discretized into n elements for computing some parameters such as area and radius r .

Once the solution was established and a computer program developed to simulate conductivity measurements in a two-phase system based on induced potentials, a test simulation was performed in a two-phase system, where one phase has medium conductivity (simulating muscle) and the other phase has very low conductivity (bone). Figure 2 shows the reconstructed conductivity map for the two proposed phases using the developed program, with the color assignment of the calculated conductivity values using a 'jetair' color map.

2.4. Conductivity to porosity relationship

Next, a simulation is carried out to determine a relationship between electrical conductivity and percentage porosity. Conductivity values for healthy bone and for porous bone are used, the conductivity of bone is 0.006 S m , muscle with 1 S m^{-1} (Mueller and Siltanen 2012); the conductivity of red bone marrow is 0.05 S m^{-1} (Chiu and Stuchly 2005); and the conductivity of blood is 0.5 S m^{-1} (Geddes and Baker 1967, Hernández 2004). Conductivity of the skin is highly variable, depending on several factors, but for this study it has a value of 0.1 S m^{-1} (De Santis *et al* 2015, Tsai *et al* 2019, Abe and Nishizawa 2021). These materials are the ones that fill the pores when bone loss occurs. Based on these values, a simulation was performed, proposing different conductivity values that correspond to different percentages of porosity, assuming a linear relationship.

The spatial configuration is shown in figure 3. Figure 3 represents square pixels as conductivity cells or elements with value σ_i . The set of elements is rounded by a circumference of radius r and n electrodes. It is very important to measure the perimeter of the measured region in the future experiments with physical measurements and obtain the value of radius, here let us r as the value. Figure 3 shows an element as a minimum measurement area .

We define the pore electrical density (PED) as the difference between one and the porous electrical density, which is a parameter that relates 100% of the porosity in the bone minus the percentage of porosity present in the measured sample. The PED represents the electrical density of the pores that fill the bone with blood and therefore measures the number of pores present in the bone. 100% of porosity

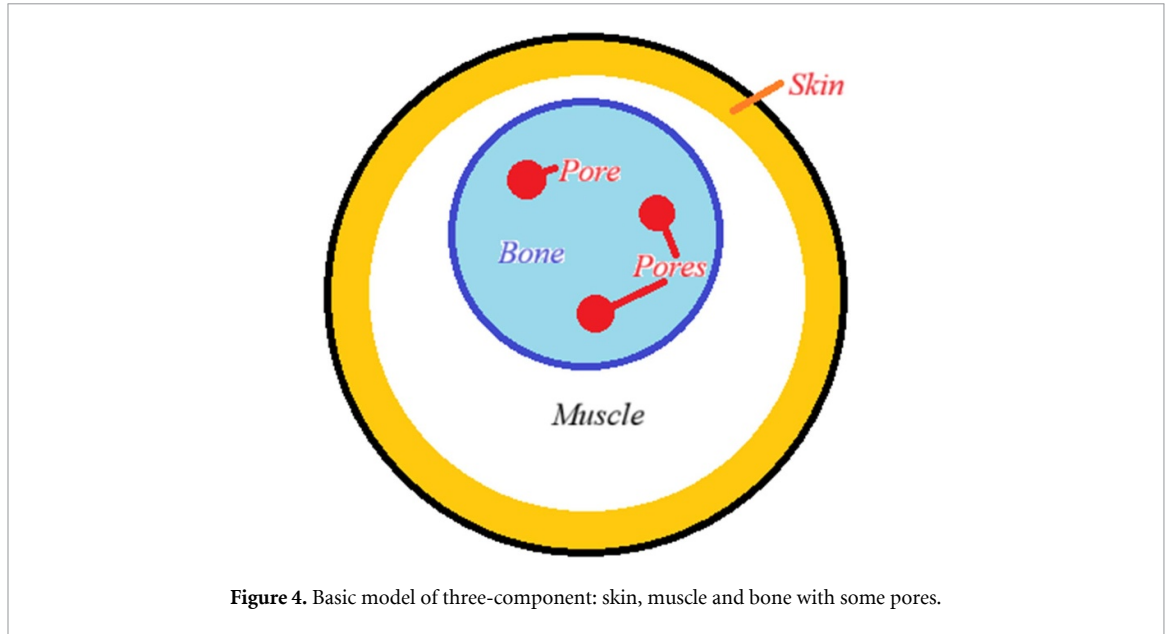


Figure 4. Basic model of three-component: skin, muscle and bone with some pores.

in a bone is 100% of conductivity value of blood and 0% pores is a total of bone conductivity values.

$$PED = 1 - BED . \quad (6)$$

In turn, the bone electrical density (BED) is defined as the ratio between the measured effective BEC (San-Pablo-Juarez *et al* 2017) and the area of the bone (AOB). A high PED value represents a low BED value, and vice versa, making these quantities inversely proportional.

$$BED = \frac{BEC}{AOB} . \quad (7)$$

The term effective is related to the isotropic behavior of conductivity. If the electrical conductivity is measured from all the electrodes and the average is obtained, then we say that it is an effective electrical conductivity.

As the units of the BEC are $S\ m^{-2}$ and the units of the AOB are m^2 , the units of the BED are $S\ m^{-3}$.

The AOB is obtained with the measurement of the perimeter of the measured region (by example the boundary around the arm or leg), equation (8), this is the number of pixels times the minimal measurement area as in equation (9),

$$AOB = \#BonePixels \cdot MMA \quad (8)$$

$$MMA = \frac{\pi r^2}{\#ofElements} . \quad (9)$$

2.5. Basic model for EIT

A simple model that includes skin, bone and muscle was used in this work. This model can be shown in figure 4.

The model of figure 4 is a proposed slice because it is very similar to an arm, leg or wrist configuration about the bones, even to a finger or other parts of the body that have a big bone respect the muscle. This configuration has little skin and a lot of bone area. Note that the pores contain blood, that is conductive.

This model was chosen for this kind of measurement because the bone is very close to the skin and there is little muscle. The more muscle there is, the higher the impedance, which increases noise and the standard deviation. This approach does not consider noise for the simulation.

The next parameters were used for simulations when the BED was computed: materials as bone ($0.006\ S\ m^{-1}$), skin ($0.1\ S\ m^{-1}$), pores with blood ($0.5\ S\ m^{-1}$) and muscle ($1\ S\ m^{-1}$); porosity ranges from 0% to 35% porosity, circular geometry with FEM triangular mesh, Ag/AgCl electrodes, mounting in a 16 electrode configuration with adjacent injection current, temperature was not considered in this

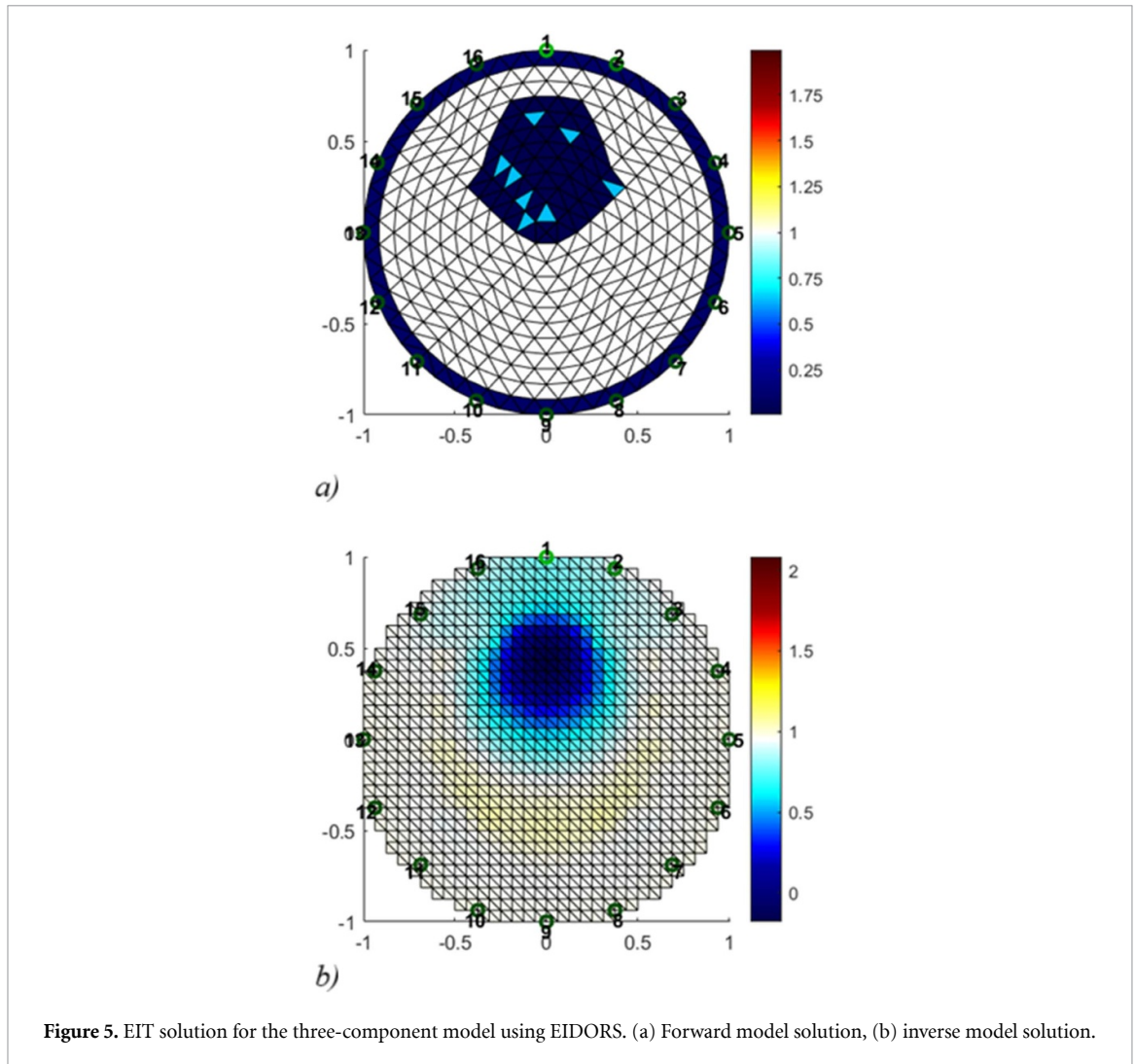


Figure 5. EIT solution for the three-component model using EIDORS. (a) Forward model solution, (b) inverse model solution.

simulation, and measurement electronics was made using electronics characteristics as current injection of 0.5 mA peak at 10 kHz, adjacent method, differential measurement amplifiers with common mode rejection ratio of 115 dB.

2.6. Other software implementations

In this work a simple backprojection method implemented in C++ is shown, but the computing of EIT can be made with more powerful tools as EIT and Diffuse Optical Tomography Reconstruction Software (EIDORS) (Adler and Lionheart 2006), using another mathematical method that solves the inverse problem as Graz consensus Reconstruction algorithm for EIT and other methods as Gauss–Newton with the finite element method. Both differential and absolute that are typical reconstructions in the EIT can be done with this software. An example of simulation with the configuration shown in figure 4 was made using EIDORS. The simulation is shown in figure 5.

Figure 5(a) shows the model that includes skin (the outer ring with low conductivity), muscle (the middle part) and bone (the object upper and centered) with a couple of pores. Figure 5(b) shows the EIT of figure 5(a), note that the reconstruction is made by using 16 electrodes and the. The main contrast is due to the bone conductivity.

2.7. Phantom

In this study, a phantom was constructed to perform a qualitative assessment of the bone image prior to acquiring measurements from a human subject. Even though this study only derives the relationship between porosity and electrical conductivity through simulation, the phantom measurements are valuable as they qualitatively ensure that the detected signal indeed corresponds to bone, rather than to any other element introducing noise.

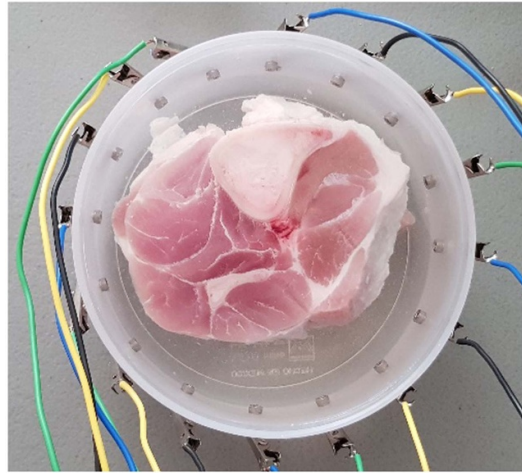


Figure 6. Pork bone in the test system.

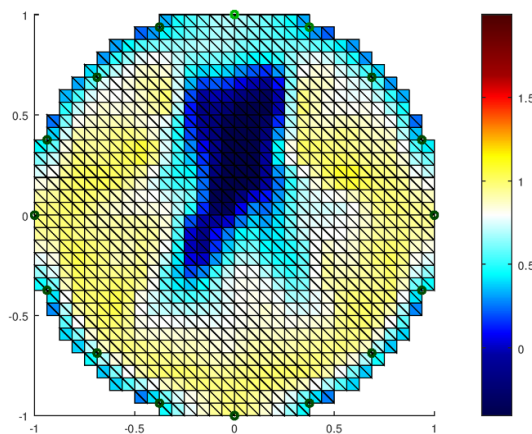


Figure 7. Conductivity of a pork bone in the test system.

The phantom consisted of measuring a sample of pork bone inside a probe cell as shown in figure 6. The results are shown in the conductivity map of figure 7, a distribution of the conductivity change of the bone, and the homogeneous material is reconstructed. Given the reconstruction for low conductivity values as those of bone, this device has the capacity to measure bone samples, case for which this work is focused.

The average value of conductivity of the measured bone was 0.009 S m^{-1} with respect to the saline water reference of 1 S m^{-1} .

Since the measurement was made with current injection from several directions in 360° it is said that this average value corresponds to a value of electrical conductivity in the bone at least qualitatively, despite the anisotropy of the bone. The phantom has an area of 0.06 m^2 with a height of 0.14 m .

3. Results

Figure 8 shows the values obtained by applying the program developed for two-phase simulation for a healthy bone sample, for a bone sample with 17% porosity, one with 26% porosity and another for 32% porosity. The root mean squared error for this simulation was of 1.78. The structural similarity index measure was 0.79. A CNR of 0.89. Results of error measurement were obtained using MATLAB (R2022b version) software (The Mathworks Inc., 2022).

Figure 8 shows the muscle conductivity, which is colored yellow (muscle conductivity), and the blue valley or sink corresponds to the bone conductivity. The results in figure 8 show a qualitative difference between the electrical conductivity of a sample without porosity and one with different porosities. The

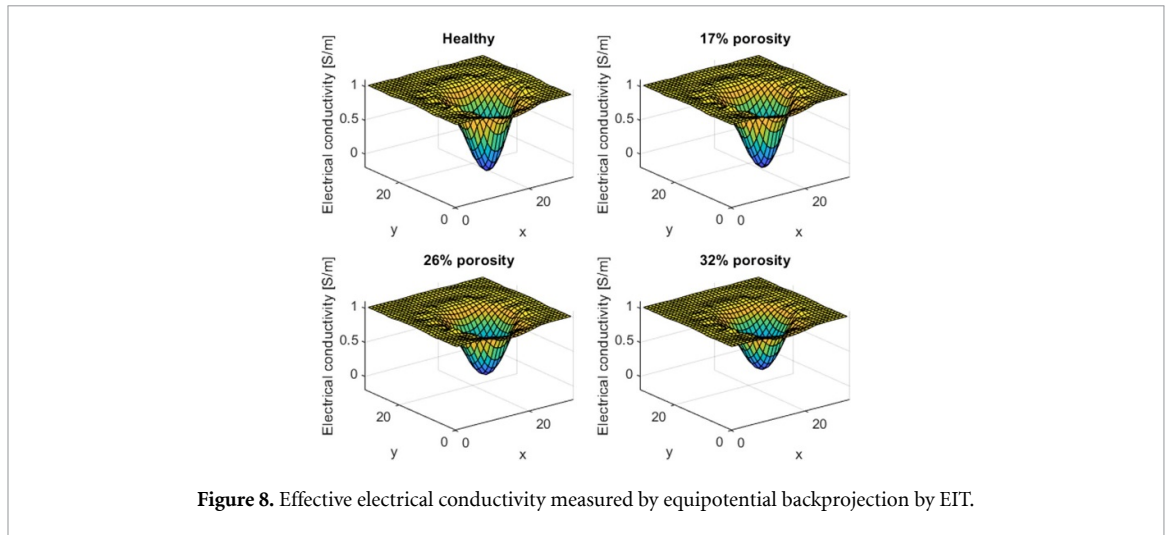


Figure 8. Effective electrical conductivity measured by equipotential backprojection by EIT.

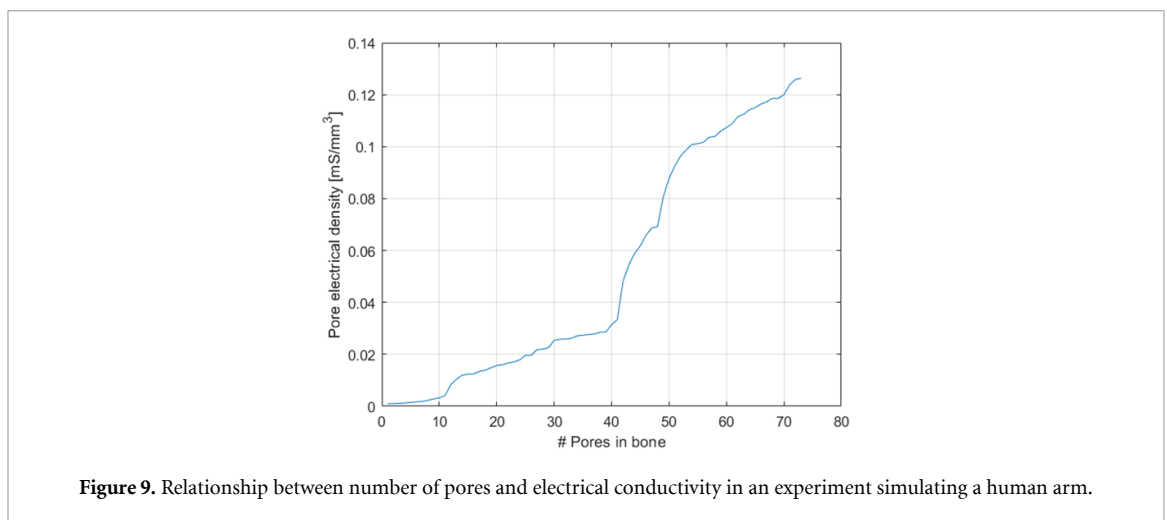


Figure 9. Relationship between number of pores and electrical conductivity in an experiment simulating a human arm.

lower the porosity, the lower the conductivity value. The higher the porosity, the higher the conductivity, demonstrating the hypothesis put forward in this work of a relationship between porosity and electrical conductivity. Plotting the conductivity against the number of pores in the simulation, the relationship in figure 8 is obtained, where a proportional, nonlinear relationship between electrical conductivity (a measure of electrical conductivity obtained using the EIT technique) and porosity can be seen. The results of figure 8 were displayed using the MATLAB (R2022b version) software (The MathWorks Inc 2022).

Once the conductivity was determined as a function of bone porosity, a mathematical relationship was obtained by numerical approximation of the curve in figure 9.

Figure 9 shows that when there are more pores, the measurement is more conductive and when there are fewer pores, less conductive. The results of figure 5 were displayed using the MATLAB (R2022b version) software (The MathWorks Inc 2022).

Figure 10 shows the third-order polynomial approximation with a correlation coefficient of 0.96. Equation (10) corresponds to the mathematical expression of a third-order polynomial that relates the percentage of porosity with the conductivity value. The results of figure 10 were displayed using the MATLAB (R2022b version) software (The MathWorks Inc 2022).

$$\%_{\text{Pore}} = 1.42E05 \cdot \text{PED}^3 - 2.98E04 \cdot \text{PED}^2 + 2.03E03 \cdot \text{PED} + 0.57. \quad (10)$$

With these data and the reference for reported BMD values (Guelman 2006), it is possible to define percentage porosity ranges that are associated with the susceptibility to osteopenia and osteoporosis. Regarding the hip, the conductivity values are only for reference, in the future, an electrode array would be used that would not perform classical tomography with a ring-shaped electrode configuration, but rather a superficial one, with an arrangement that penetrates up to the bone without surrounding it, by

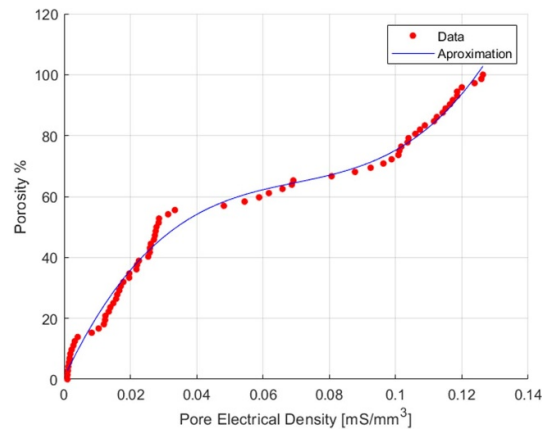


Figure 10. Polynomial approximation to calculate the percentage of porosity in bone using electrical conductivity.

Table 1. Assignment of a percentage of porosity with respect to the electrical conductivity values in bone.

Osteoporosis score	BMD (mg cm^{-2})	Porosity %	Pore electrical density (mS mm^{-3})	Bone electrical density (mS mm^{-3})
Normal	950–1400	00.0–32.1	0.0005–0.0177	0.9823–0.9995
Osteopenia	650–940	32.8–53.5	0.0178–0.0401	0.9599–0.9822
Osteoporosis	500–640	54.2–64.2	0.0402–0.0715	0.9285–0.9598

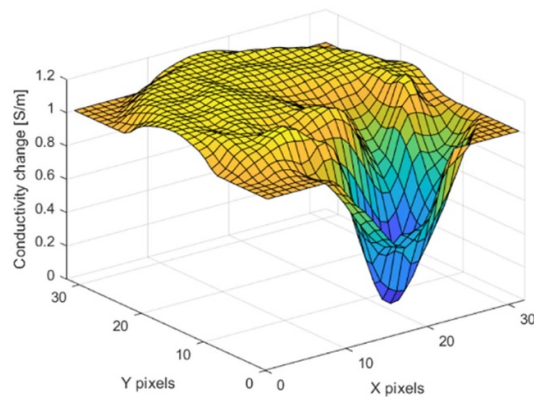


Figure 11. Phantom results for measured electrical conductivity.

example for bon hip conductivity measurement. One advantage of measuring the hip using EIT is that the bones are very close to the skin, with almost no fat or muscle.

Table 1 shows reported BMD values relative to the ranges corresponding to the experiment performed. This demonstrates that the electrical conductivity of bone *in vivo* is inversely related to BMD. Table 1 shows proposed threshold values for determining three porosity levels: healthy, osteopenia, or osteoporosis, according to the standards used for BMD. Therefore, the proposed method allows for a pre-diagnosis of osteoporosis based on conductivity measurements and can be used on a large scale as a prevention method.

An advantage of using PED instead of BED is that the comparison between porosity levels is easier to observe and to measure using the graph of figure 10.

So, using the table 1 scores, it is possible to measure the levels of porosity in bone. This is the new method proposed to measure bone porosity based on *in vivo* electrical conductivity measurement.

Finally, a bone conductivity measurement test was carried out but using a cut of meat (pork) as a phantom, as on figure 6. Figure 11 shows a tank result, note that the meat is formed of both cortical and cancellous bone, lean and fatty meat. Given the reconstruction for low conductivity values as those of bone, this device has the capacity to measure bone samples, case for which this work is focused. It

should be noted that the meat sample contains no blood, as it is intended for human consumption, so blood values does not appear at the measurements.

As an example, the percentage of porosity for the phantom bone will be Normal because the mean conductivity was 0.009 S m^{-1} , and according to table 1, this Porosity corresponds to the percentage of porosity.

This method does not aim to replace the gold standard for measuring bone porosity, but rather to provide a tool for pre-diagnosis and porosity monitoring, so the results of this method can be considered for future studies and developing of instrumentation to measure bone porosity *in-situ* or monitoring a porosity evolution in the bone.

4. Conclusions

A three-phase computational model for skin, muscle and bone was developed to simulate electrical conductivity measurements based on the porosity or conductivity change of one of the phases.

It was shown that the electrical conductivity of bone is directly related to the percentage of porosity and BMD at least in a basic simulation that includes three-component model, with bone and muscle.

The proposed method allows threshold values to be obtained for determining porosity at three levels: healthy bone, osteopenia, or osteoporosis.

It was shown that electrical conductivity varies according to bone porosity, and a correlation between conductivity measurements and bone density was obtained, creating a new theoretical method for detection of osteoporosis.


Data availability statement

All data that support the findings of this study are included within the article (and any supplementary information files).

Acknowledgments

We thank the Instituto Politecnico Nacional (IPN) for its funding through Grant SIP20240493 and SIP20253618.

Author contributions

Miguel-Ángel San-Pablo-Juárez  0000-0002-1093-3870

Investigation (lead), Software (lead), Supervision (lead), Validation (lead), Visualization (lead), Writing – original draft (lead)

Maria-Montserrat Oropeza-Saucedo  0009-0003-0039-0766

Investigation (supporting), Resources (supporting)

Eduardo Morales-Sánchez  0000-0002-0855-5460

Investigation (equal), Writing – review & editing (equal)

References

- Abe Y and Nishizawa M 2021 Electrical aspects of skin as a pathway to engineering skin devices *APL Bioeng.* **5** 041509
- Adler A and Lionheart W R 2006 Uses and abuses of EIDORS: an extensible software base for EIT *Physiol. Meas.* **27** S25–S42
- Ain K, Putra A P, Rahma O N, Hikmawati D, Rahmatillah A and Che Abdullah C A 2024 Electrical impedance spectroscopy as a potential tool for detecting bone porosity *Sens. Actuators A* **370** 115252
- Barber D and Brown B 1984 Applied potential tomography *J. Phys. E* **17** 723–33
- Baroncelli G 2008 Quantitative ultrasound methods to assess bone mineral status in children: technical characteristics, performance, and clinical application *Pediatr. Res.* **63** 220–8
- Chiu R S and Stuchly M A 2005 Electric fields in bone marrow substructures at power-line frequencies *IEEE Trans. Biomed. Eng.* **52** 1103–9
- De Santis V, Chen X L, Laakso I, Chou C K, Ruggera P S and Hirata A 2015 An overview of safety assessment of electromagnetic fields exposure from human skin perspective *Biomed. Phys. Eng. Express* **1** 015201
- Geddes L and Baker L E 1967 The specific resistance of biological material—a compendium of data for biomedical engineers and physiologists *Med. Biol. Eng.* **5** 271–93
- Guelman R 2006 La densitometría ósea en los muy ancianos. ¿T-score? ¿Z-score? *Actual. Osteol.* **2** 36–38 (available at: <https://ojs.osteologia.org.ar/ojs33010/index.php/osteologia/issue/view/55>)
- Hernández F 2004 *Caracterización de sangre por espectroscopía de impedancia eléctrica, medición de la difusión térmica del suero Tesis de maestría*(Universidad Autónoma de Nuevo León (UANL))

- Holder D 2005 *Electrical Impedance Tomography: Methods, History and Applications* (Institute of Physics Publishing)
- Ireta F 2012 *Estudios de descalcificación ósea mediante técnicas de espectroscopia de impedancia eléctrica Tesis doctoral* (CICATA-IPN Querétaro, Instituto Politécnico Nacional)
- Mautalen C, Vega E, Gonzáles D, Carrilero P, Otaño A and Silberman F 1995 Ultrasound and dual x-ray absorptiometry densitometry in women with hip fracture *Calcif. Tissue Int.* **57** 165–8
- Mishra M B, Mishra S and Mishra R 2011 Dental care in the patients with bisphosphonates therapy *Int. J. Dent. Clin.* **3** 60+ (available at: <https://link.gale.com/apps/doc/A346926672/AONE?u=anon~fad0d2c4&sid=googleScholar&xid=bbcc02bc>)
- Molinari M 2003 High fidelity imaging in electrical impedance tomography *PhD dissertation*
- Mueller J and Siltanen S 2012 *Linear and Nonlinear Inverse Problems with Practical Applications* (Society for Industrial and Applied Mathematics (SIAM))
- Muñoz-Torres M, Varsavsky M and Avilés-Pérez M D 2010 Osteoporosis. Definición. *Epidemiología Rev. Osteoporos. Metab. Miner.* **2** s5–s7/Supl(3) (available at: www.revistadeosteoporosisymetabolismomineral.com/magazines/139/show)
- North American Menopause Society 2010 Management of osteoporosis in postmenopausal women: 2010 position statement of The North American Menopause Society *Menopause* **17** 25–54
- Reza-Albarrán A A 2016 Osteoporosis *Gac. Med. Mex.* **152** 84–89 (available at: <https://dialnet.unirioja.es/revista/17546/V/152?anualidad=2016>)
- Rosell F J 1989 Tomografía de impedancia eléctrica para aplicaciones médicas *PhD Dissertation*
- San-Pablo-Juárez M A, Morales-Sánchez E, Ireta-Moreno F, Ávalos-Zúñiga R and González-Barbosa J J 2017 Method for measuring bone density through the electrical conductivity calculated by electrical impedance tomography *Rev. Mex. Ing. Bioméd.* **38** 492–506
- Santosa F and Vogelius M 1990 A backprojection algorithm for electrical impedance imaging *SIAM J. Appl. Math.* **50** 216–43
- The MathWorks Inc 2022 MATLAB version 9.13.0 (R2022b) Update 2 (The MathWorks Inc) (available at: www.mathworks.com)
- Tsai B, Xue H, Birgersson E, Ollmar S and Birgersson U 2019 Dielectrical properties of living epidermis and dermis in the frequency range from 1 kHz to 1 MHz *J. Electr. Bioimpedance* **10** 14–23
- Turner C, Peacock M, Timmerman L, Neal J and Johnston C Jr 1995 Calcaneal ultrasonic measurements discriminate hip fracture independently of bone mass *Osteoporos. Int.* **5** 130–5
- Vauhkohonen P 2004 Image reconstruction in three-dimensional electrical impedance tomography *Doctoral dissertation* University of Kuopio
- Vijay A, Shankar N, Liges C and Anburajan M 2011 Evaluation of osteoporosis using CT image of proximal femur compared with dual energy x-ray absorptiometry (DXA) as the standard *Proc. 3rd Int. Conf. on Electronics Computer Technology (ICECT)*